Section 1

Atmospheric data assimilation schemes, analysis and initialization, data impact studies, observing system experiments

Impact of observations on the AROME-France convective-scale data-assimilation system

Pierre Brousseau and Gérald Desroziers
CNRM-GAME, Météo-France and CNRS
42 av Coriolis 31057 Toulouse, France
Pierre.brousseau@meteo.fr

The theory of linear statistical estimation, based on the minimization of the estimation error variance, provides an estimate of the true state of the atmosphere, the analysis, as a combination of two sources of information, the background and the observations, weighted with error covariances that represent the uncertainty associated to each kind of information. It can be shown that, if observation and background error covariance matrices are well specified, the analysis error covariance matrix is given by $\mathbf{A} = \mathbf{B} - \mathbf{KHB}$ where **B**, **K** and **H** respectively stand for the assumed background error covariance matrix, the Kalman gain matrix and the linearized observation operator. The total variance reduction provided by the assimilation of the observation $r=\mathrm{Tr}(\mathbf{B})-\mathrm{Tr}(\mathbf{A}) = \mathrm{Tr}(\mathbf{KHB})$ is a measurement of the ability of a data assimilation (DA) system to pull the analysis from the background with respect to the observations (Tr stands for the trace of a matrix). A direct estimate of the variance reduction $\mathrm{Tr}(\mathbf{KHB})$ is not possible in practice in an operational variational DA, since neither **B** nor **K** are explicitly known. Desroziers et al. (2005) proposed to estimate the variance reduction, and the contributions of the different observation types, with a randomization method in the global ARPEGE 4D-Var. This method, implemented in the AROME-France convective-scale 3D-Var scheme (Brousseau et al., 2013) allows one to investigate observation impact depending on the control variable field, model levels, date, analysis time, and spatial scales considered.

The observations with the largest impact in the AROME-France 3D-Var system are given by aircraft (for temperature and wind fields) and radar (specific humidity and wind fields) observations in the middle and high troposphere, in accordance with the vertical distribution of these observations (Figure 1). Screen-level measurements (2 m temperature, 2 m relative humidity and 10 m wind) are the main contributors at the lowest atmospheric levels. These large impact values are explained by the number of these observations assimilated at each analysis time. On a rainy day, aircraft, radar and screen-level observations account for respectively 22%, 30% and 18% of the total account of assimilated observations. One can note that it is possible to evaluate the impact of an observation of a given physical quantity (resp. at a given model level) on the analyzed field of an other physical quantity (resp. on other levels) through the **B** matrix cross- (resp. vertical) correlations. The total variance and the different observation contributions are also evaluated depending on the spatial scale of the analyzed fields: most of variance reduction concerns length scales above 100 km with a maximum around 500-800 km. Only the radar measurements, with an horizontal density of 15 km, contribute to the variance reduction at scales lower than 100 km.

This *a posteriori* diagnostic provides rich and useful information on the impact of the different observation types on the analysis. It is not intended to replace Observing System Experiments but rather to complement them to optimize the design of observing networks and their use in various data assimilation systems, particularly at convective scale.

References:

Desroziers G., Brousseau P. and Chapnik B. 2005. Use of randomization to diagnose the impact of observations on analyses and forecasts. Quart. J. Roy. Meteor. Soc. 13 : 2821–2837.

Brousseau P., Desroziers G., Bouttier F. and Chapnik B. 2013. *A posteriori* diagnostics of the impact of observations on the AROME-France convective-scale data-assimilation system. Quart. J. Roy. Meteor. Soc. Submitted

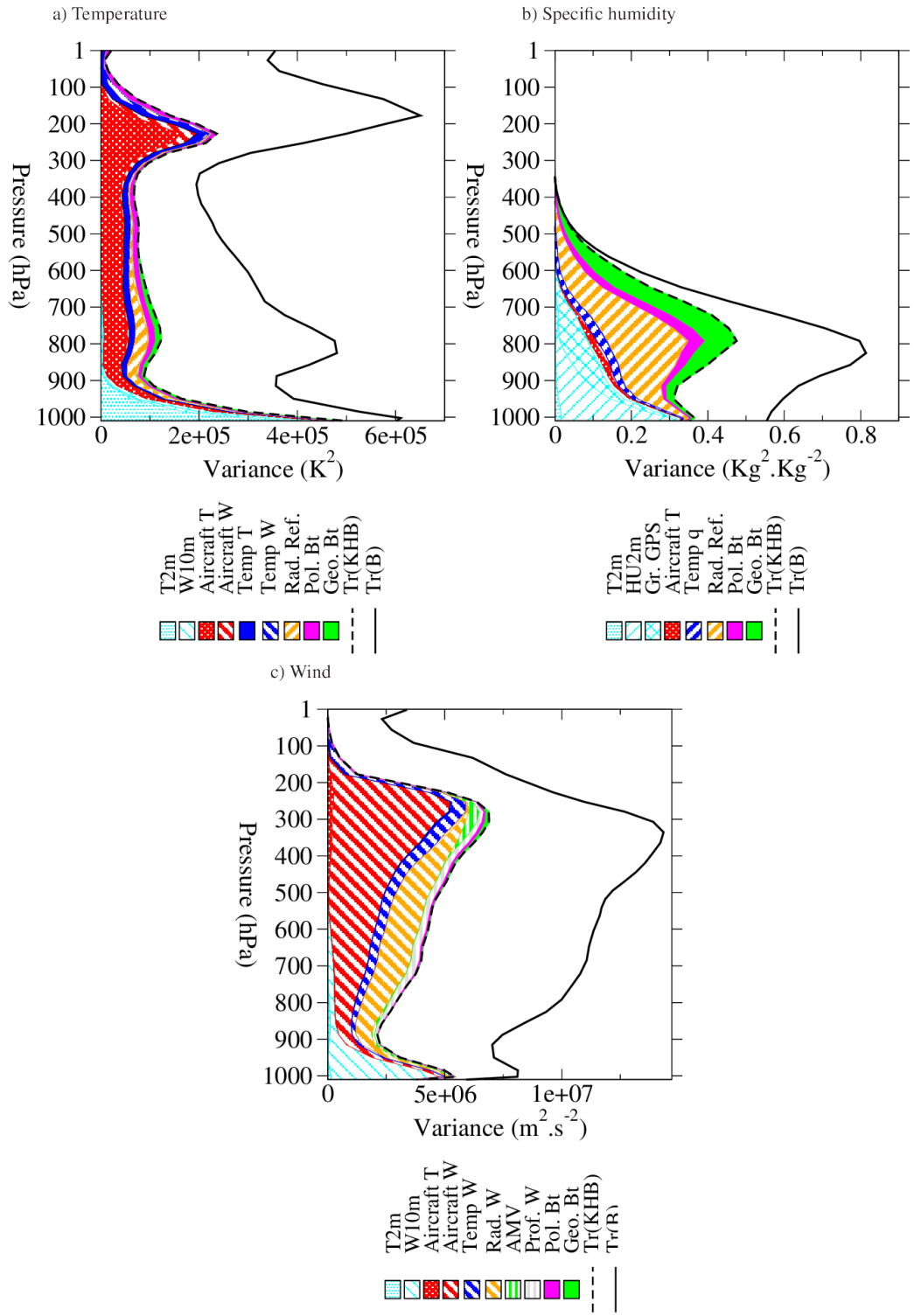

*Figure 1: Vertical profile of the background error total variance (Tr(**B**): plain line), variance reduction (Tr(**KHB**): dashed line) and observation subset contributions to Tr(**KHB**) (shaded areas) averaged on 3 May 2010 for temperature (a), specific humidity (b) and wind (c). T2m: 2 m temperature; W10m: 10 m wind; Aircraft T, W: aircraft temperature, wind; Temp T, q, W: radio-sounding temperature, specific humidity, wind;Rad. Ref., W: radar reflectivity, doppler wind; Pol. Bt: brightness temperature on board polar platform; Geo. Bt: brightness temperature on board geostationary platform; HU2m: 2 m relative humidity;Gr. GPS: Ground-based GPS zenith total delay; AMV: atmospheric motion vector; Prof. W: wind profiler.*

Improving Estimation of Model Uncertainty in the NCEP Global Ensemble Forecast System

Jeffrey S. Whitaker, Thomas M. Hamill, and Philip Pegion

NOAA Earth System Research Lab, Boulder, Colorado USA
Contact: Jeffrey.s.whitaker@noaa.gov

A major focus of our assimilation and ensemble prediction group at NOAA ESRL / PSD continues to be to develop improved ensemble-based data assimilation and ensemble prediction methods, primarily but not exclusively based on existing NCEP models and assimilation methods, e.g., the GFS (Global Forecast System) model, the GEFS (Global Ensemble Forecast System) and the hybrid EnKF/GSI (Ensemble Kalman Filter/Grid-point Statistical Interpolation) data assimilation system. Our research for 2013-2014 will focus on several aspects, including the testing the impact of cycling the hybrid system at higher resolution during Northern Hemisphere tropical cyclone season using an experimental higher-resolution, semi-Lagrangian version of the GEFS, and possibly using a 4D-Ensemble-Var approach (pending adequate computing resources). We also continue to experiment with improved and existing methods for simulating model uncertainty, including operational methods at NCEP (the STTP method, Stochastic Total Tendency Perturbations), the SPPT method at ECMWF (Stochastically perturbed parameterized tendencies), Stochastic Kinetic Energy Backscatter, a perturbed boundary layer relative humidity approach, and potentially other methods in the future. Our intent is to determine both whether these methods, when cycled in the ensemble data assimilation scheme and in free ensemble forecasts improve the assimilations and ensemble forecasts respectively. Our intent is to provide evidence to help NCEP determine whether changes to their operational data assimilation and ensemble prediction methods are warranted.

Recommended Nomenclature for EnVar Data Assimilation Methods

Andrew C. Lorenc

Met Office, Exeter EX1 3PB, UK. andrew.lorenc@metoffice.gov.uk

At the WMO THORPEX Data Assimilation and Observing Systems Working Group (DAOS WG) meeting in 2011, the group felt there was a need for a common terminology for hybrid ensemble variation methods. The issue was discussed again at the 2012 meeting. The recommendations below attempt to represent the views expressed. We have tried to select a non-ambiguous terminology based on the most common existing established usage.

1. **En** should be used to abbreviate Ensemble (not Ens), as it is in the EnKF.

2. Hyphenated abbreviations (4D-Var, 3D-Var) were standardised by Ide *et al.* (1997) (and some journals), but they are not usually used in names for EnKF methods. The hyphen may be omitted in new names.

3. **4D-Var** or **4DVAR** are so well established that, even with a prefix or suffix, they should only be used for methods using a forecast model and its adjoint. Methods not using an adjoint method should use a name which does not make them seem variants of 4D-Var. In particular we discourage the terminology En4DVAR used by Liu *et al.* (2008, 2009) to mean an an algorithm designed not to use an adjoint model. Instead we recommend **4DEnVar** as being more distinct from 4DVAR, and more similar to the 4DEnKF of Hunt *et al.* (2004). A prefix to 4D-Var can qualify it as in 4 or 7 below, but it should not change the basic 4D-Var method.

4. **hybrid** should describe the covariances used, not the method. E.g. "hybrid 3DVAR" (Wang *et al.*, 2008a,b) and "hybrid 4D-Var" (Clayton *et al.*, 2012) are Var methods using a combination of climatological and ensemble covariances. Pure 4DEnVar, using only ensemble covariances, should not be described as a hybrid method.

5. **EnVar** may be used without qualification (as EnKF is), if there is no need to stress the specific details of the implementation, to mean a variational method using ensemble covariances. For example a hybrid-4DEnVar may be simply described as EnVar.

6. The **EnKF** and its specific flavours (e.g. ETKF) generate ensembles as part of their algorithm. **EnVar**, like 3D-Var or 4D-Var, may generates a single best estimate and not an ensemble. Papers should make it clear if an ensemble is generated, e.g. Bonavita *et al.* (2012) use EDA as nomenclature for an Ensemble of [4D-Var] Data Assimilations.

7. Following the style of hybrid-4D-Var, it would be natural to use En4DVar for 4D-Var using ensemble covariances; Zhang and Zhang (2012) used E4DVar for such a system. However En4DVAR was used by Liu *et al.* (2008, 2009) for something else. So until recommendation 3 is generally adopted, it may be safer to use 4D-Var-Ben or 4D-Var-Benkf (Buehner *et al.*, 2010a,b; Fairbairn *et al.*, 2013).

8. Ensemble covariances are modified to reduce sampling error for elements where the true correlation is assumed to be near zero. This localization (also spelt as localisation) is most simply defined in terms of horizontal distance (Hamill *et al.*, 2001), but can also be done in the vertical and in spectral space (Buehner and Charron, 2007). Related methods modify the observation selection for a local analysis (Ott *et al.*, 2004). A key feature of such **localization** techniques is that they leave unchanged aspects of the ensemble covariance which are not being specifically localised. It is possible to reduce the effect of the localisation so far that it has no effect; in this case the ensemble covariance is unaltered. This is in contrast to indirect use of ensemble covariances to derive coefficients in a parametric covariance model (e.g. Bonavita *et al.* (2012)). If that model happens to give local covariances then fitting it has a similar effect of removing sampling error for distant covariances, but this should not be called localisation since it changes the covariances everywhere – there is no way to recover the original ensemble covariance.

References

Bonavita M, Isaksen L, Holm E. 2012. On the use of EDA background error variances in the ECMWF 4D-Var. *Q. J. R. Meteorol. Soc.* **138**: 1540–1559, doi:10.1002/qj.1899.

Buehner M, Charron M. 2007. Spectral and spatial localization of background-error correlations for data assimilation. *Q. J. R. Meteorol. Soc.* **133**(624): 615–630, doi:10.1002/qj.50, URL `http://dx.doi.org/10.1002/qj.50`.

Buehner M, Houtekamer PL, Charette C, Mitchell HL, He B. 2010a. Intercomparison of variational data assimilation and the ensemble Kalman filter for global deterministic NWP. part i: Description and single-observation experiments. *Mon. Weather Rev.* **138**: 1550–1566, doi:10.1175/2009MWR3157.1.

Buehner M, Houtekamer PL, Charette C, Mitchell HL, He B. 2010b. Intercomparison of variational data assimilation and the ensemble Kalman filter for global deterministic NWP. part ii: One-month experiments with real observations. *Mon. Weather Rev.* **138**: 1567–1586, doi:10.1175/2009MWR3158.1.

Clayton AM, Lorenc AC, Barker DM. 2012. Operational implementation of a hybrid ensemble/4D-Var global data assimilation system at the Met Office. *Q. J. R. Meteorol. Soc.* **on-line**: 16pp, doi:10.1002/qj.2054.

Fairbairn D, Pring SR, Lorenc AC, Roulstone I. 2013. A comparison of 4D-Var with various flow-dependent data assimilation methods. *Q. J. R. Meteorol. Soc.* **accepted**.

Hamill TM, Whitaker JS, Snyder C. 2001. Distance dependent filtering of background error covariance estimates in an ensemble Kalman filter. *Mon. Weather Rev.* **129**: 2776–2790.

Hunt B, Kalnay E, Kostelich E, Ott E, Patil D, Sauer T, Szunyogh I, Yorke J, Zimin A. 2004. Four-dimensional ensemble Kalman filtering. *Tellus A* **56**(4): 273–277.

Ide K, Courtier P, Ghil M, Lorenc A. 1997. Unified notation for data assimilation: Operational, sequential and variational. *J. Met. Soc. of Japan* **75**: 181–189.

Liu C, Xiao Q, Wang B. 2008. An ensemble-based four-dimensional variational data assimilation scheme. part i: Technical formulation and preliminary test. *Mon. Weather Rev.* **136**: 3363–3373, doi:10.1175/2008MWR2312.1.

Liu C, Xiao Q, Wang B. 2009. An ensemble-based four-dimensional variational data assimilation scheme. part ii: Observing System Simulation Experiments with advanced research WRF (ARW). *Mon. Weather Rev.* **137**: 1687–1704, doi:10.1175/2008MWR2699.1.

Ott E, Hunt BR, Szunyogh I, Zimin AV, Kostelich EJ, Corazza M, Kalnay E, Patil DJ, Yorke JA. 2004. A local ensemble Kalman filter for atmospheric data assimilation. *Tellus A* **56A**: 415–428, doi:10.1111/j.1600-0870.2004.00076.x.

Wang X, Barker DM, Snyder C, Hamill TM. 2008a. A hybrid ETKF-3DVAR data assimilation scheme for the wrf model. part i: Observing system simulation experiment. *Mon. Weather Rev.* **136**: 5116–5131, doi:10.1175/2008MWR2444.1.

Wang X, Barker DM, Snyder C, Hamill TM. 2008b. A hybrid ETKF-3DVAR data assimilation scheme for the WRF model. part ii: Real observation experiments. *Mon. Weather Rev.* **136**: 5132–5147, doi:10.1175/2008MWR2445.1.

Zhang M, Zhang F. 2012. E4DVar: Coupling an ensemble Kalman filter with four-dimensional variational data assimilation in a limited-area weather prediction model. *Mon. Weather Rev.* **140**(2): 587–600.

DISPLACED ENSEMBLE VARIATIONAL ASSIMILATION EXPERIMENT USING BRIGHTNESS TEMPERATURES OF MICROWAVE IMAGER

Seiji ORIGUCHI, Kazumasa AONASHI and Kozo OKAMOTO
Meteorological Research Institute, Tsukuba, Japan
E-mail; origuchi@mri-jma.go.jp

1. Introduction

Displacement erorrs in large-scale appear between the precipitation distributions of the ensemble forecast results and the actual observation data in many cases. In the recent study, the experiment of data assimilation about typhoon's case was performed using ensemble forecast results that corrected displacement error by observation data, and we can know that those results were the analysis results of high precision compared with case of no correction (Aonashi and Eito (2011)). In the present study, we selected heavy rain event within the Baiu frontal zone that was appeared diurnal variation in the precipitation regions for weak rain (The Baiu frontal zone extended from southern part of the East China Sea to southern sea of Japan between 12 June 2009 and 13 June 2009). For this event, at first, we performed displacement error correction (DEC) of the ensemble forecast results (first guesses) using brightness temperatures (TBs) of Microwave Imager (MWI) on the satellite. Next, we performed the experiment of ensemble-based variational assimilation (EnVA) from the displaced first guesses, and we compared with ensemble mean before DEC, ensemble mean after DEC and EnVA analysis value.

2. Method of DEC

We calculated displacement error ($\vec{d}$) from TBs (Y) of MWI and ensemble mean ($\bar{X}^f$) using the following cost function (Hoffman and Grassotti (1996)).

$$J_d = \frac{1}{2\sigma_o^2}\{Y - H(\bar{X}^f(\vec{d}))\}^T\{Y - H(\bar{X}^f(\vec{d}))\} + \frac{1}{2\sigma_d^2}|\vec{d}|^2$$

H : Forward operator, σ_o : Observation error, $\sigma_o^2 = 10K^2$
σ_d : Scale of displacement error, $\sigma_d = 150km$

Next, we corrected physical elements, radiational calculated TBs for each members and ensemble mean from the optimized displacement error ($\vec{d} = \tilde{d}$). DEC scheme was considered horizontal direction only.

3. Experiment of EnVA

We calculated analysis value of ensemble mean ($\bar{X}^a$) from TBs (Y), displaced ensemble mean ($\bar{X}^f(\tilde{d})$) and displaced each ensemble members ($\bar{X}_i^f(\tilde{d})$) using the following cost function.

$$J_X = \frac{1}{2}\{\bar{X}^a - \bar{X}^f(\tilde{d})\}^T(P^f)^{-1}\{\bar{X}^a - \bar{X}^f(\tilde{d})\} + \frac{1}{2\sigma_o^2}\{Y - H(\bar{X}^a)\}^T\{Y - H(\bar{X}^a)\}$$

Where, back ground error covariance (P^f) consists of the displaced ensemble forecast error, and its covariance is implemented by using flow-dependency localization. In this experiment, we used the vertical polarized waves of the lower frequency three channels of 10, 19 and 21GHZ for the reasons that the horizontal polarized waves was the large sensibility for variation of wind speed over the sea and higher frequency components had the large error in the calculation of cloud resolving model and forward operator of non-spherical solid precipitation particles (Aonashi and Eito (2011)).

4. Results of Experiment

At first, we performed ensemble forecast in settings as resolution is 5km, horizontal grid size is 400×400, total members is 51 (CNTL and perturbative 50 members), and we compared with the results of ensemble mean, ensemble mean after DEC and EnVA analysis value. Where, Fig 3(a) and (b) show the precipitation intensity and the updrafts of ensemble mean before DEC at FT=14 (Validtime: 02UTC 13 June 2009), Fig3(c) and (d) show same as in Fig3(a) and (b) but of ensemble mean after DEC, Fig3(e) and (f) show same as in Fig3(a) and (b) but of EnVA analysis value respectively. Physical elements were moved using the estimated displacement error vectors by the DEC scheme (Fig2). Precipitation regions of ensemble mean after DEC were corrected mainly around the Amami and the Okinawa islands compared with ensemble mean before DEC, and it approached actual precipitation distribution (Fig1). Entirely homogeneus updraft regions were moved mainly toward the Amami and the Okinawa islands by the DEC scheme. Updrafts of EnVA analysis value were enhanced mainly around the Amami and the Okinawa islands compared with ensemble mean after DEC, and precipitation amounts also increased. Precipitation amounts of EnVA analysis value were consistent with the Radar observation data (Fig1). Next, in order to evaluate the impact of precipitation, we performed the extented 6hr forecast ensemble mean, ensemble mean after DEC and EnVA analysis value at FT=14 as initial values. As a result, the extended forecast using EnVA analysis value was the best result in the three forecast cases. These results indicate the effectivity of DEC and EnVA for the severe event of the Baiu frontal zone.

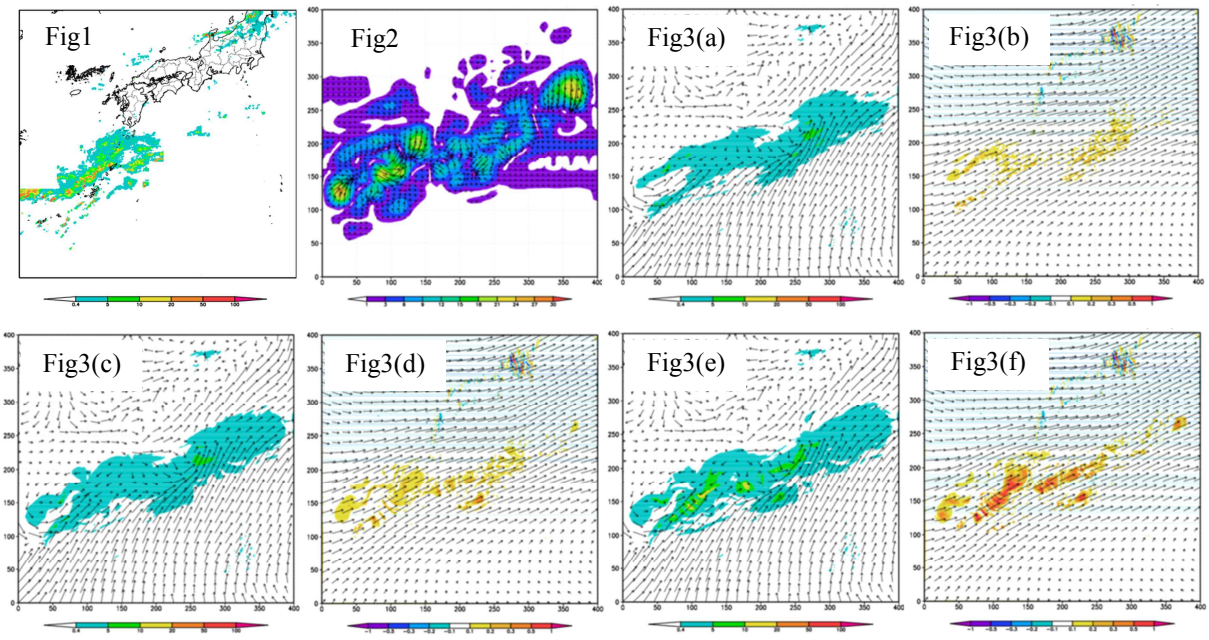

Fig1: Radar data (mm/hr) of JMA. Fig2: The estimated displacement error vectors by the DEC scheme. Fig3: (a) and (b) show the precipitaion intensity and the updrafts of ensemble mean before DEC at FT=14 respectively. (c) and (d) show same as in (a) and (b) but of ensemble mean after DEC respectively. (e) and (f) show same as in (a) and (b) but of EnVA analysis value respectively.

References

Hoffman, R. N., and C. Grassotti, 1996: A Technique for Assimilating SSM/I Observations of Marine Atmospheric Storms: Tests with ECMWF Analyses. *J. Appl. Meteor.*, **35**, 1177-1188.

Aonashi, K., and H. Eito, 2011: Displaced Ensemble Variational Assimilation Method to Incorporate Microwave Imager Brightness Temperatures into a Cloud-resolving Model. *J. Meteor. Soc.* Japan, **89**, 175-194.

Acknowledgement

A part of this research has been funded by MEXT Strategic Programs for Innovative Research (SPIRE).

Recent Updates on the Usage of GNSS RO Data in JMA's Operational Global Data Assimilation System

Hiromi Owada and Koichi Yoshimoto
Numerical Prediction Division, Japan Meteorological Agency
E-mail: howada@naps.kishou.go.jp

1. Introduction

The Japan Meteorological Agency (JMA) began assimilating Global Navigation Satellite System (GNSS) Radio Occultation (RO) refractivity data into its operational global NWP system on March 22, 2007, and revisions to this process were implemented in the system on December 18, 2012. The major updates are as follows:

- Additional use of refractivity data from TerraSAR-X and C/NOFS and resumption of GRACE-A refractivity data assimilation
- Updates of observation operators and elimination of the bias correction procedure

A bias correction procedure had been implemented in the pre-processing of RO data due to the presence of systematic biases in the tropical and polar regions. As the biases were reduced via updates of the observation operators, the correction procedure was eliminated. The updates are described in detail in the next section.

Observation system experiments for the new assimilation configuration incorporating these updates showed improved analysis and forecasting of temperature and sea surface pressure, especially in the Southern Hemisphere. Most of the improvements were brought about by the observation operator updates.

2. Updates and related impacts

JMA began assimilating RO refractivity data from GRACE-A, TerraSAR-X and C/NOFS in addition to data from Metop-A and COSMIC with the implementation of new observation operators. The number of assimilated RO data increased threefold relative to the previous operation.

Two major changes were applied to the observation operators. One was an improvement of the interpolation algorithm used for the conversion of height information. In previous operation, vertical interpolation for the computation of background refractivity values was designed on a geometric height scale. Accordingly, calculation for the conversion of geopotential height to geometric height was required for each model grid point to seek two levels between which the observation was located. The previous algorithm lacked accuracy because latitude dependence was not considered in the calculation of gravitational acceleration. Against this background, a revised method incorporating consideration of latitude dependence was introduced into the updated operators. This approach also has the advantage of reducing computational cost because height conversion is unnecessary for model grid points. The other major change was a modification of tangent linear and adjoint operators for the computation of pressure perturbation. The previous operators produced increments of only temperature and water vapor for the levels surrounding the observation. As consideration of pressure perturbation results in increments to sea surface pressure as well as temperature and water vapor, it plays an important role in the improvement of sea surface pressure analysis.

Observation system experiments for the new assimilation configuration were performed for the two months of August 2011 and January 2012. The control experiment (CNTL) had the same configuration as the previous operational global system, and the test experiment (TEST) included the above-mentioned updates, which were newly introduced into the operational system.

Figure 1 shows the mean and standard deviation of fractional normalized Metop-A refractivity differences between observations (without bias correction) and model simulations as a function of geometric height in three latitudinal bands for August 2011. Observations above 30 km (shown in grey) were not used in either experiment due to the presence of biases between observations and model simulations. In the CNTL experiment, there was a positive bias in the tropics and negative biases in the Arctic and Antarctic. In the TEST experiment, the biases were clearly reduced compared to those of the CNTL experiment. Figure 2 shows the monthly average of analyzed sea surface pressure differences between TEST and CNTL. Large differences were seen especially around the Antarctic. The effect of RO data assimilation is noticeable in this region, where surface weather observation stations are sparse. The increments in the TEST experiment were brought about by the new operators incorporating perturbation of pressure.

Acknowledgements

The authors would like to thank GFZ for providing GRACE-A and TerraSAR-X data, EUMETSAT for providing Metop-A data, USAF for providing C/NOFS data and NSPO and UCAR for providing COSMIC data.

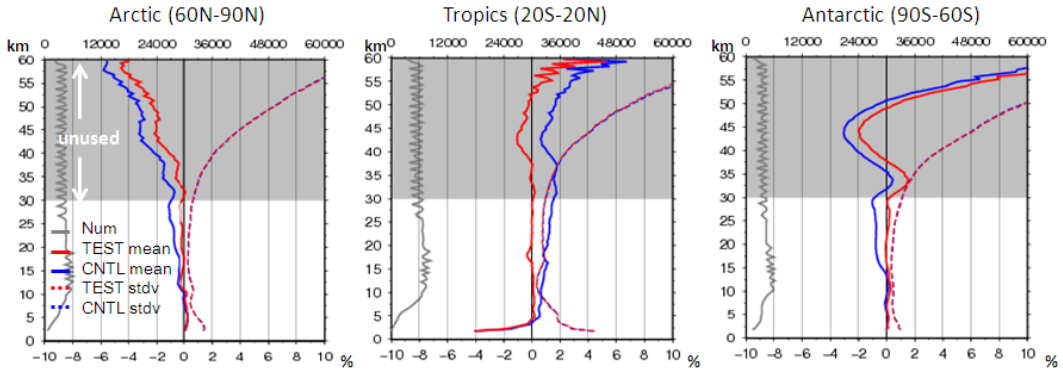

Figure 1: Mean and standard deviation of fractional refractivity differences ((O − B) / B * 100) between Metop-A observations (O) and model simulations (B) as a function of geometric height in the TEST and CNTL experiments for August 2011

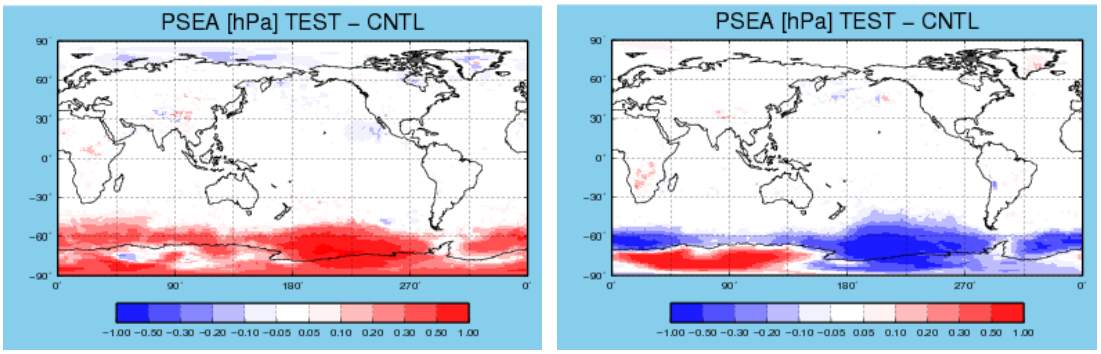

Figure 2: Monthly average of analyzed sea surface pressure differences between TEST and CNTL for August 2011 (left) and January 2012 (right)

Data Assimilation Experiments of Tornado occurring on 6th May 2012

*[1]Hiromu SEKO, [1]Kazuo SAITO, [2]Tadashi TSUYUKI, [2]Masaru KUNII and [3]Takemasa MIYOSHI
[1]Meteorological Research Institute/JAMSTEC, [2]Meteorological Research Institute, [3]RIKEN
*hseko@mri-jma.go.jp

1. Introduction

Since numerical forecasts or analyses of local heavy rainfalls or tornadoes have errors, it is difficult to predict them accurately. Especially, generation points of thunderstorms in weak convergence areas are sensitive to initial conditions. To express the thunderstorms that cause local heavy rainfalls or tornadoes, probabilistic forecasts based on ensemble predictions are desired. The ensemble prediction is also expected to reduce the miss rate of forecasts because it provides many possible scenarios of severe phenomena. The convection cells that generate the severe phenomena and environments such as low-level convergence should be reproduced simultaneously. In this presentation, a tornado generated on 6th May 2012 in the Kanto Plain was reproduced by using a two-way nested-LETKF (Local Ensemble Transform Kalmar Filter) system with horizontal resolutions of 2 km and 15 km, which expressed convection cells and environments. Downscaling forecasts with the horizontal grid intervals of 350 m and 50 m that can create intense vortices were also performed. The factors for the generations of intense vortices that were investigated by the outputs of downscale experiments are shown.

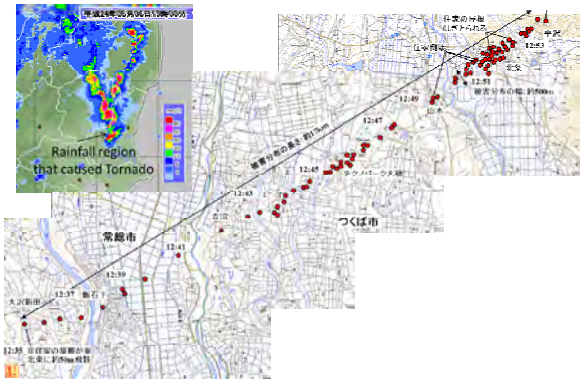

Fig. 1. Rainfall regions that were obtained by the JMA operational radar (upper left). The damage caused by the southernmost tornado. *http://www.jma.go.jp/jma/press/1205/11c/120511tsukuba_tornado.pdf.)*

2. Observed Futures of Tornadoes

On 6th May 2012, three tornadoes occurred in the Kanto plain. The southernmost tornado that was generated at the southern tip of the convection band (Fig. 1) was observed by the Meteorological Research Institute (MRI)'s Doppler radar, and high resolution deterministic forecasts were conducted by the MRI *(http://www.jma.go.jp/jma/press/1205/11c/120511tsukuba_tornado.pdf.)*. A vortex associated with the southernmost tornado, which was captured by the MRI's Doppler radar, was generated at the southern part of the filament-like rainfall region (Fig. 2). A deterministic forecast with the horizontal grid interval of 50 m indicated that a tornado was generated in a super-cell rainfall. A moist airflow with a water vapor mixing ratio of over 12 g/kg was supplied into the convection band, in which the tornado was generated.

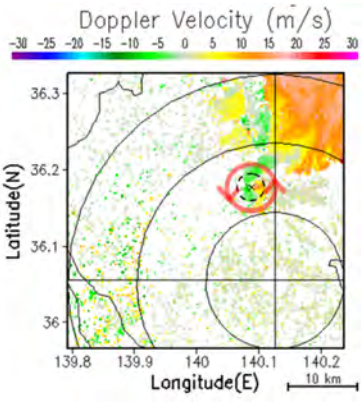

Fig. 2. Radial wind observed by the Doppler Radar of MRI. Red arrows indicate the vortex. *(http://www.jma.go.jp/jma/press/1205/11c/120511tsukuba_tornado.pdf.)*

3. Outline of experiments using the Nested LETKF system

To obtain the initial conditions of the Japan Meteorological Agency non-hydrostatic model (JMANHM) with the horizontal grid interval of 350 m (NHM-350) and 50 m (NHM-50), the nested-LETKF system, which was composed of two LETKFs (Miyoshi and Aranami, 2006), was used (Fig. 3). The outer LETKF with a grid interval of 15 km assimilates the convectional data of the Japan Meteorological Agency. The assimilation window was 6 hours. An inner

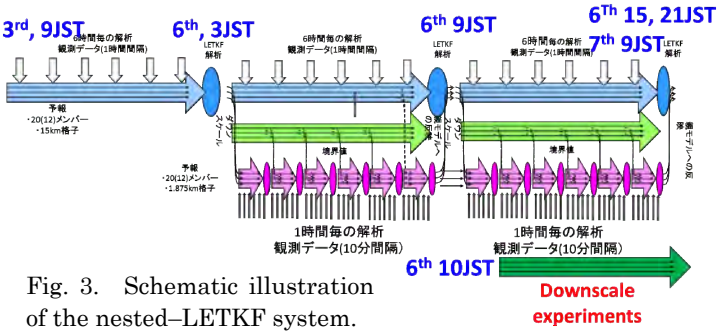

Fig. 3. Schematic illustration of the nested–LETKF system.

LETKF was deployed in the Kanto region in the outer LETKF. The grid interval of the inner LETKF is about 2 km. The assimilation window was 1 hour. Results of the inner LETKF were reflected in the outer LETKF every 6 hours. The Outer and Inner LETKFs were begun at 9 JST 3rd and 3 JST 6th, respectively. Also, downscale experiments using NHM-350 and NHM-50 were performed from 10:30 JST and 11:20 JST, respectively. The initial and boundary conditions of NHM-350 and NHM-50 were produced from the outputs of the Inner LETKF and NHM-350, respectively. In this study, the assimilation data that was used in the Japan Meteorological Agency was used in the Inner LETKF and high resolution data, such as Doppler radar data or GPS water vapor data, was not used in the assimilation of the Inner LETKF.

4. Results of ensemble forecasts

A rainfall region that extended northward and moved northeastward was reproduced in all ensemble members of NHM-350. Intense vortices in which the vertical vorticity exceeded 0.1 (1/s) were generated in 10 of 12 ensemble members. Namely, the occurrence probability of intense vortices in this case was 83 %. Positions and durations depend on the ensemble members. Tornadoes occurred in 3 areas (Fig. 4), which were the same as the observations though they were shifted northward by 10 km. A comparison of environments in NHM-350 forecasts around the vortices in their mature stages shows that the large vertical shear of the horizontal wind and low-level humid airflow made the duration of the vortices longer (Fig. 5). A comparison of initial conditions between the ensemble members, in which intense vortices were generated and not generated, indicated that a small moister region from the south extended their durations (not shown).

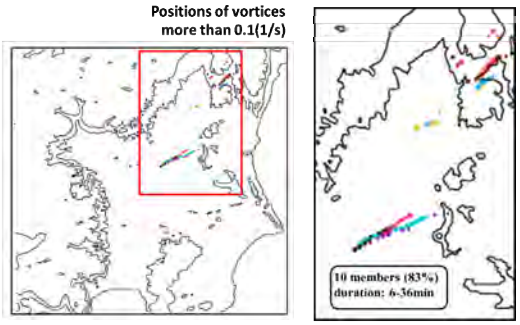

Fig. 4. Positions of vortices more than 0.1 (1/s) reproduced by NHM-350.

As for the ensemble forecast of NHM-50, which was calculated by the K-computer (Fig. 6), various structures of vortices, such as a vortex that had two minimum pressure points (not shown), were generated. These comparisons provide the generation mechanisms of tornadoes.

5. Summary and future plan

The vortices of tornadoes occurring on 6th May 2012 were reproduced by the nested LETKF system, which is under development to reproduce the environments and convection cells. An ensemble forecast of 60 members is now being conducted by the K-computer. Results of ensemble forecasts are to be used to investigate the generation mechanisms of tornadoes. Doppler radar data and GPS water vapor data, which are expected to improve the forecasts of convection cells, will be used as assimilation data of the Inner LETKF.

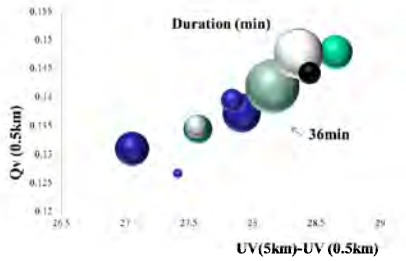

Fig. 5. Relationship between the duration of vortices, vertical wind shear, and low-level water vapor that was reproduced by NHN-350. Sizes of spheres indicate the durations of vortices.

Acknowledgements

Parts of the results were obtained by using the K computer at the RIKEN Advanced Institute for Computational Science (Proposal number hp120282).

References

Miyoshi, T. and K. Aranami 2006: Applying a Four-dimensional Local Ensemble Transform Kalman Filter (4D-LETKF) to the JMA Nonhydrostatic Model (NHM). *SOLA*, **2**, 128-131.

Seko, H., T. Tsuyuki, K. Saito, and T. Miyoshi, 2013, Development of a two-way nested-LETKF system for cloud-resolving model, *Data Assimilation for Atmospheric, Oceanic and Hydrological Applications (Vol. II)*, p 489-507.

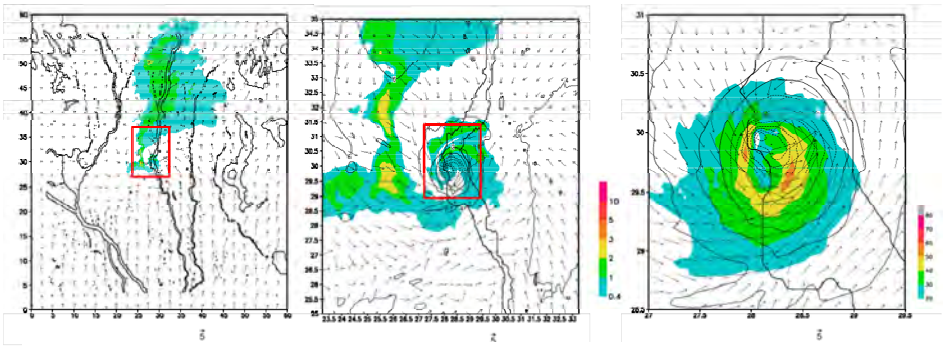

Fig. 6. (a) Rainfall regions (colored regions) and horizontal wind (vectors) near surface of ensemble member #004 that were reproduced by NHM-50. (b) and (c) Magnified figures of (a). Colored region in (c) indicates wind velocity.